Original article

MOLECULAR METABOLISM

Mechanisms underlying prorenin actions on hypothalamic neurons implicated in cardiometabolic control

Soledad Pitra [1], Yumei Feng [2], Javier E. Stern [1,*]

ABSTRACT

Background: Hypertension and obesity are highly interrelated diseases, being critical components of the metabolic syndrome. Despite the growing prevalence of this syndrome in the world population, efficient therapies are still missing. Thus, identification of novel targets and therapies are warranted. An enhanced activity of the hypothalamic renin-angiotensin system (RAS), including the recently discovered prorenin (PR) and its receptor (PRR), has been implicated as a common mechanism underlying aberrant sympatho-humoral activation that contributes to both metabolic and cardiovascular dysregulation in the metabolic syndrome. Still, the identification of precise neuronal targets, cellular mechanisms and signaling pathways underlying PR/PRR actions in cardiovascular- and metabolic related hypothalamic nuclei remain unknown.
Methods and results: Using a multidisciplinary approach including patch-clamp electrophysiology, live calcium imaging and immunohistochemistry, we aimed to elucidate cellular mechanisms underlying PR/PRR actions within the hypothalamic supraoptic (SON) and paraventricular nucleus (PVN), key brain areas previously involved in cardiometabolic regulation. We show for the first time that PRR is expressed in magnocellular neurosecretory cells (MNCs), and to a lesser extent, in presympathetic PVN neurons (PVN_{PS}). Moreover, we show that while PRR activation efficiently stimulates the firing activity of both MNCs and PVN_{PS} neurons, these effects involved AngII-independent and AngII-dependent mechanisms, respectively. In both cases however, PR excitatory effects involved an increase in intracellular Ca^{2+} levels and a Ca^{2+}-dependent inhibition of a voltage-gated K^{+} current.
Conclusions: We identified novel neuronal targets and cellular mechanisms underlying PR/PRR actions in critical hypothalamic neurons involved in cardiometabolic regulation. This fundamental mechanistic information regarding central PR/PRR actions is essential for the development of novel RAS-based therapeutic targets for the treatment of cardiometabolic disorders in obesity and hypertension.
© 2016 The Author(s). Published by Elsevier GmbH. This is an open access article under the CC BY-NC-ND license (http://creativecommons.org/licenses/by-nc-nd/4.0/).

Keywords Prorenin receptor; Sympathetic; PVN; SON; Angiotensin; Potassium

1. INTRODUCTION

It is well-established that the brain renin-angiotensin system plays a critical role in hydromineral and cardiovascular regulation, and that an elevated central RAS contributes to cardiovascular diseases, particularly neurogenic hypertension [1–3]. In addition to its canonical role in cardiovascular function, the RAS has recently emerged as a critical mediator of the hypothalamic control of body weight and metabolic functions [4,5]. An increase RAS activity, resulting in elevated levels of AngII and AngII type 1a receptors (AT1a) in the brain, has been reported both in obese humans and animal models [4,6–8]. Moreover, increasing central RAS activity, either genetically or pharmacologically, decreased body weight by inhibiting food intake and elevating energy expenditure [9–12].
Hypertension and obesity are highly interrelated diseases, being critical components of the metabolic syndrome. Diet-induced obesity in humans and rodents is associated with increased prevalence of hypertension [13–15], and several studies implicate an altered central RAS in obesity-induced hypertension [16–18]. Furthermore, neurogenic forms of hypertension caused by an elevated brain RAS activity display several metabolic disturbances [5]. Importantly, a mechanistic interaction between energy balance-related signals (e.g., leptin) and the central RAS in the functional regulation of sympathetic nerve activity has been reported both in health and disease conditions [19,20]. Finally, AngII is a pro-inflammatory factor [21], and inflammation within the hypothalamus has been associated both with hypertension and obesity [16,22–25]. Collectively, these results suggest that an altered brain RAS activity could be a common mechanism underlying both cardiovascular and energy balance changes in the metabolic syndrome.
Neurons within the paraventricular nucleus of the hypothalamus (PVN) are well suited to mediate the effects of the central RAS on cardiovascular and metabolic regulation. Parvocellular presympathetic neurons, via projections to the brainstem and spinal cord [26], influence

[1]Department of Physiology, Medical College of Georgia, Augusta University, United States [2]Departments of Pharmacology, Physiology and Cell Biology, Center for Cardiovascular Research, University of Nevada School of Medicine, United States

*Corresponding author. Department of Physiology, Medical College of Georgia, Augusta University, 1120 15th Street, CA-3137, Augusta, GA 30912, United States.
E-mail: jstern@augusta.edu (J.E. Stern).

Received July 13, 2016 • Revision received July 26, 2016 • Accepted July 27, 2016 • Available online 4 August 2016

http://dx.doi.org/10.1016/j.molmet.2016.07.010

 © 2016 The Author(s). Published by Elsevier GmbH. This is an open access article under the CC BY-NC-ND license (http://creativecommons.org/licenses/by-nc-nd/4.0/).

food intake, energy expenditure and blood pressure [27–29]. Magnocellular neurosecretory cells (MNCs) that project to the posterior pituitary (also present in the supraoptic nucleus, SON) [26], release oxytocin and vasopressin onto the circulation. These hormones, in addition to their well-established effects on fluid and electrolyte homeostasis, also influence metabolic function and food intake [30–34]. All the components of the RAS needed for the local generation of angiotensin peptides are present within the SON and PVN [35], including two of the most novel players, namely prorenin (PR) and its receptor (PRR) [36–38]. Binding of PR to PRR stimulates the catalytic activity of the receptor, converting angiotensinogen (AGT) to angiotensin I and II [36,38]. In addition, interaction of PR with PRR initiates intracellular signaling pathways, including mitogen-activated protein kinases (MAPK) and extracellular signal-regulated kinases 1 and 2 (ERK1/2) [39–41]. Thus, the PR/PRR complex can mediate both AngII-dependent and independent effects.

An altered RAS activity within the SON/PVN leads to aberrant sympatho-humoral outflows characteristic of both hypertension and the metabolic syndrome. For example, an increased PRR expression was reported in the SON and PVN in hypertensive mice and rats [42,43], while brain-targeted PRR knockdown decreased blood pressure, sympathetic tone and plasma VP levels in these rodents [38,42]. Importantly, both AngII-dependent [44] and independent [43], mechanisms where shown to mediate effects of PRR in these nuclei. Furthermore, deletion of AT1a receptors in the PVN of high-fat diet obese mice increased food intake, decreased energy expenditure and decreased systolic blood pressure [45], supporting a key role for AT1a receptors in the PVN in the regulation of cardiometabolic function during obesity. While PR and PRR in adipose tissue have been recently implicated in the development of obesity and obesity-induced hypertension [46,47], their contribution to hypothalamic control metabolic function, both in health and disease is much less understood.

Despite all this evidence, the identification of precise neuronal targets, cellular mechanisms and signaling pathways underlying PR-mediated sympatho-humoral activation within cardiovascular and metabolic related brain centers remain unknown. This fundamental mechanistic information regarding central PR/PRR actions is critical before this signaling unit can become an efficient and novel therapeutic target for the treatment of cardiometabolic disorders.

The degree of sympathetic and hormonal outputs from the SON/PVN is dependent on neuronal activity in these nuclei, which is in turn determined by the combined actions of intrinsic (ion channels) and extrinsic (neurotransmitters) factors. Thus, it is reasonably to speculate that PR/PRR actions within the SON/PVN to stimulate sympatho-humoral activation are mediated by increasing membrane excitability and evoking firing activity in these neuronal populations. Surprisingly however, there have been no studies in the literature thus far that investigated this, nor explored the precise underlying cellular mechanisms by which PR mediates neurohumoral activation within the brain. Here, we used a multidisciplinary experimental approach including patch-clamp electrophysiology, live confocal calcium imaging and immunohistochemistry to elucidate cellular mechanisms underlying PR/PRR actions within the SON/PVN.

2. METHODS

2.1. Ethical approval

All procedures were performed in agreement with guidelines of the Augusta University Institutional Animal Care and Use Committee and were approved by the committee. Male heterozygous transgenic eGFP-VP Wistar rats (4–6 weeks old) were used [48]. Rats were housed in rooms with constant temperature of 22–24 °C and under a controlled light/dark cycle (12 h: 12 h), with normal rat chow and drinking water ad libitum.

2.2. Retrograde tracing

To identify presympathetic PVN neurons for patch-clamp or immunohistochemistry, rhodamine-labeled microspheres (Lumaflor) or cholera toxin B (CTB; 1%; List Biological Laboratories, 400 nl), respectively, were microinjected into the RVLM, a major brainstem sympathetic center. Coordinates used starting from bregma: 12 mm caudal along the lamina, 2 mm medial lateral, and 8 mm ventral as previously described [49]. The location of the tracer was verified histologically. Animals were used for electrophysiological or immunohistochemical studies 3–4 days after surgery.

2.3. Slice preparation

Hypothalamic brain slices were prepared according to methods previously described [50,51]. Briefly, rats were anesthetized with pentobarbital (50 mg/kg ip); brains dissected out and hypothalamic coronal slices (240 μm) containing the SON/PVN were cut in an oxygenated ice-cold artificial cerebrospinal fluid (aCSF), containing in mM: 119 NaCl, 2.5 KCl, 1 $MgSO_4$, 26 $NaHCO_3$, 1.25 NaH_2PO_4, 20 D-glucose, 0.4 ascorbic acid, 2 $CaCl_2$, and 2 pyruvic acid; pH 7.3; 295 mOsm. When indicated a 0 Ca^{2+} ACSF (in which Ca^{2+} was replaced by Mg^{2+}, and EGTA 2 mM was added) was used. Slices were placed in a holding chamber containing aCSF and kept at room temperature until used.

2.4. Electrophysiology

Hypothalamic slices were transferred to a recording chamber and superfused with continuously bubbled (95% O_2–5% CO_2) aCSF (30 °C–32 °C) at a flow rate of ~3.0 ml/min. Thin-walled (1.5-mm OD, 1.17-mm ID) borosilicate glass (G150TF-3; Warner Instruments, Sarasota, FL) was used to pull patch pipettes (3–5 MΩ) on a horizontal micropipette puller (P-97; Sutter Instruments, Novato, CA). The internal solution contained the following (in mM): 135 potassium gluconate, 0.2 EGTA, 10 HEPES, 10 KCl, 0.9 $MgCl_2$, 4 Mg^{2+}ATP, 0.3 Na^{+}GTP and 20 phosphocreatine (Na^{+}); pH was adjusted to 7.2–7.3 with KOH. When indicated, a Cs+ -based internal solution (in mM: 135 Cs MS, 0.2 EGTA, 10 HEPES, 10 TEACl, 0.9 MgCl) was used. Recordings were obtained from fluorescently labeled PVN_{PS} neurons and from eGFP-VP neurons with an Axopatch 200B amplifier (Axon Instruments, Foster City, CA), using a combination of fluorescence illumination and infrared differential interference contrast (DIC) videomicroscopy. Recordings of eGFP-VP neurons in the PVN were restricted to the core of the lateral magnocellular (LM) subnuclei, which contains only magnocellular VP neurons [26] and were further characterized as magnocellular neurons electrophysiologically, based on the presence of a transient outward rectification (not shown), a membrane property expressed in magnocellular but not parvocellular SON/PVN neurons. The voltage output was digitized at 16-bit resolution, 10 kHz and was filtered at 2 kHz (Digidata 1440A; Axon Instruments). In voltage-clamp mode, ramp-evoked currents were leaked-substracted. Data were discarded if the series resistance was not stable throughout the entire recording (>20% change) [50,51]. Mouse prorenin (2.5 nM, Anaspec) was pressure applied through a picospritzer pipette (5 s). Focal application of ACSF, used as a control for a potential mechanical effect on the recorded neuron, failed to evoke a change in any of the parameters measured (not shown). All drugs, with the exception of Losartan (LKT Laboratories) and the PRR antagonist PRO20 (generated in the laboratory of Dr. Feng, UNR) [52], were purchased from Sigma–Aldrich. Mean firing activity and membrane potential values were calculated

 © 2016 The Author(s). Published by Elsevier GmbH. This is an open access article under the CC BY-NC-ND license (http://creativecommons.org/licenses/by-nc-nd/4.0/).

from a 1 min period before drug application and in a 1 min period around the peak effect, using Clampfit (Axon Instruments) or Mini-Analysis (Synaptosoft) software. Neurons were considered responsive if a change in firing rate frequency of at least 25% was observed between basal period and drug administration.

In voltage clamp mode, current density was determined by dividing the current amplitude by the cell capacitance, obtained by integrating the area under the transient capacitive phase of a 5 mV depolarizing step pulse, in voltage clamp mode. Neurons in each experiment were recorded from 2 to 8 rats.

2.5. Confocal calcium imaging

Neurons were loaded through the patch pipette with Fluo-5F pentapotassium salt (50 μM; Invitrogen), as previously described [53]. Imaging was conducted using the Andor Technology Revolution system (iXON EMCCD camera with the Yokogawa CSU 10, confocal scanning unit). Fluorescence images were acquired at a rate of 4 Hz, using an excitation light of 488 nm and emitted light at >495 nm (Fluo-5F). The fractional fluorescence (F/F0) was determined by dividing the fluorescence intensity (F) within a region of interest by a baseline fluorescence value (F0) determined from 50 images before PR application [54]. Data were analyzed using ImageJ software.

2.6. Immunohistochemistry

Rats were anesthetized with pentobarbital (50 mg/kg ip) and perfused transcardially with 4% paraformaldehyde in 0.01 M PBS. Brains were then removed, and coronal slices (20 μm) containing the SON/PVN were cut and incubated overnight with a combination of the following primary antibodies: rabbit anti-PRR, that targets the N-terminal of the receptor (1:400; generated in the laboratory of Dr. Feng, UNR) [42]; rabbit anti-PRR, that targets the C-terminal of the receptor (1:200; Abcam); goat anti-CTB (1:1000; List Biological Laboratories); guinea pig anti-VP (1:20000; Bachem); guinea pig anti-OT (1:50000; Bachem). Incubation in primary antibodies was followed by specific fluorescently labeled secondary antibodies (1:250; Jackson ImmunoResearch Laboratories) for 4 h. The specificity of the anti-PRR antibody generated in the laboratory of Dr. Feng was validated in a neuron-specific PRR knockout mouse [44], as well as in cell lines using PRR-shRNA [42]. Slices were then rinsed and visualized using a Zeiss LSM 510 Confocal Microscope System (Carl Zeiss, Oberkochen, Germany) [55]. Twenty consecutive optical focal planes (2 μm interval) were acquired from sections containing the middle level of the lateral magnocellular subnucleus of the PVN and the middle part of the SON (Bregma = −1.40 to −1.80) and a projection image was generated as a single section. OT and VP immunoreactive MNCs from the SON and the PVN subnuclei, as well as retrogradely-labeled PVN_{PS} neurons were individually traced within their respective acquisition channels using a freehand tool within ImageJ software (1.47v, National Institutes of Health, USA). The channel was then switched to the one containing the PRR immunoreactivity, and the mean PRR immunofluorescence intensity within the traced cell was obtained and expressed in arbitrary units ranging from 0 (absolute black) to 4095 (absolute white). Background intensity was calculated from adjacent areas and was subtracted from all images. A mean value of all sampled neurons was obtained and used for comparisons.

2.7. Statistical analysis

All values are expressed as means ± SE. Student's paired *t* tests were used to compare the effects of drug treatment. One-way ANOVA tests with Bonferroni post hoc tests were used as needed. Differences were considered significant at $p < 0.05$ and n refers to the number of cells. All statistical analyses were conducted using GraphPad Prism (GraphPad Software, San Diego, CA).

3. RESULTS

3.1. Prorenin stimulates firing activity of MNCs and PVN_{PS} neurons

Whole-cell patch-clamp recordings were obtained from identified MNCs and presympathetic PVN neurons (PVN_{PS}), and measurements of changes in firing rate in response to PR were obtained. As shown in Figure 1, focal application of PR (2.5 nM, 5 s) to MNCs increased their firing discharge ($p = 0.001$; $n = 12$; responsive cells: 12/12). Interestingly, a stronger effect, which however did not reach statistical significance, was observed in all MNCs from the SON when compared to those of the PVN (SON: Δ firing rate: 3.8 ± 1.0 Hz vs. PVN 1.5 ± 0.3 Hz; $p = 0.06$; $n = 6$ each). A comparable PR-evoked increased firing activity was observed in PVN_{PS} neurons ($p = 0.001$; $n = 12$; responsive cells: 9/12).

Changes in firing activity occurred with a delay of 1.8 ± 0.5 min from PR application in MNCs, and 3.1 ± 0.5 min in PVN_{PS} neurons. In most cases, as shown in Figure 1, PR effects did not washout, at least within the time our recordings lasted.

A subset of MNCs was identified as VP neurons ($n = 6$), based on the expression of eGFP [48]. In this group, PR significantly increased their firing discharge (before PR 0.8 ± 0.1 Hz vs. after PR 2.3 ± 0.3 Hz; $p = 0.002$; responsive cells: 6/6), an effect that was not different from that observed in non-identified MNCs ($p > 0.3$). Thus, subsequent experiments were carried out in MNCs, with only some of them being identified eGFP-VP cells.

To determine whether the increased firing activity triggered by PR involved an underlying membrane depolarization, PR was applied to a subset of MNCs and PVN_{PS} neurons that were hyperpolarized to ∼ −10 mV from spike threshold, so that measurements of Vm could be obtained in the absence of action potentials. We found that PR application caused a significant membrane depolarization in both groups of neurons: MNCs: +1.5 ± 0.2 mV, $p < 0.0001$; $n = 8$; PVN_{PS}: +2.7 ± 0.8 mV $p = 0.03$; $n = 5$.

3.2. Prorenin excitatory effects involve different signaling mechanisms in MNCs and PVN_{PS} neurons

To determine whether PR excitatory effects on SON and PVN neurons (a) required activation of the PRR, and (b) if they were AngII-dependent, we repeated experiments in the presence of a selective PRR antagonist (PRO20), or in the presence of the AT1 receptor blocker losartan. Given that PR effects did not wash-out within our recording period (see above), PR effects in these set of experiments were tested directly in the presence of either blocker. As shown in Figure 2, PR-evoked increase in firing discharge in MNCs was blocked by bath application of a PRR antagonist (PRO20; 250 nM; before PR: 1.1 ± 0.5 Hz vs. after PR: 0.5 ± 0.3 Hz; $p = 0.1$; $n = 5$; responsive cells: 1/5; Figure 2A), but persisted in the presence of the AT_1 receptor (AT_1R) blocker, losartan (50 μM; before PR: 0.5 ± 0.1 Hz vs. after PR: 2.2 ± 0.5 Hz; $p = 0.002$; $n = 17$; responsive cells: 15/17). Conversely, in PVN_{PS} neurons the PR excitatory effect was completely blocked by losartan (before PR: 0.6 ± 0.3 Hz vs. after PR: 0.3 ± 0.2 Hz; $p = 0.1$; $n = 6$; responsive cells: 1/6; Figure 2B). Moreover, while a tendency for an excitatory effect was still observed in 5/6 neurons in the presence of PRO20, this did not reach statistical significance (before PR: 1.0 ± 0.2 Hz vs. after PR: 1.7 ± 0.4 Hz; $p = 0.09$; $n = 6$). These results suggest that while PR actions are primarily PRR-mediated and *AngII-independent* in MCNs, they are predominantly *AngII-dependent* in PVN_{PS} neurons. Interestingly, regardless of the underlying mechanism involved, when

 © 2016 The Author(s). Published by Elsevier GmbH. This is an open access article under the CC BY-NC-ND license (http://creativecommons.org/licenses/by-nc-nd/4.0/).

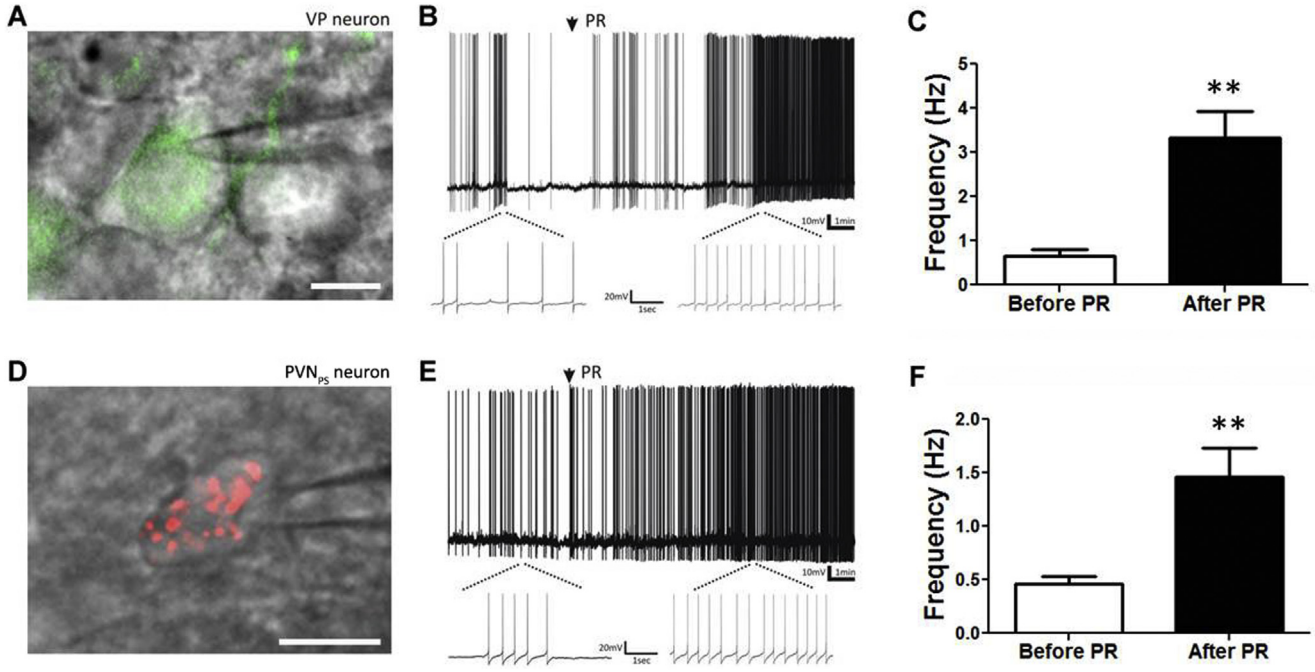

Figure 1: PR increases the firing activity of SON/PVN MNCs and PVN$_{PS}$ neurons. A, Representative example of a patched eGFP-VP neuron, showing that focal application of PR (2.5 nM, 5 s) increased its firing activity (**B**). **C**, Summary data showing mean firing frequencies (Hz) before and after PR application in MNCs (n = 12). **D**, Representative example of a patched PVN$_{PS}$ neuron, showing that focal application of PR (2.5 nM, 5 s) increased its firing activity (**E**). **F**, Summary data showing mean firing frequencies (Hz) before and after PR application in PVN$_{PS}$ neurons (n = 12). **p < 0.01. Scale bars: 10 μm.

PR excitatory effects were blocked in both neuronal types, a tendency for a masked inhibitory effect was unveiled. This phenomenon however was not further investigated in the present work.

Generation of angiotensin peptides by PR/PRR requires the availability of the substrate angiotensinogen (AGT). Thus, to assess whether diminished availability of AGT could be a factor contributing to the lack of an AngII-mediated PR effect in MNCs, AGT (1 μg/ml) was added to the bathing solution when recording from these neurons. PR still triggered an increase in firing discharge in MNCs in the presence of high AGT levels (AGT 1.5 ± 0.3 Hz vs. AGT PR 3.1 ± 0.5 Hz; p = 0.03;

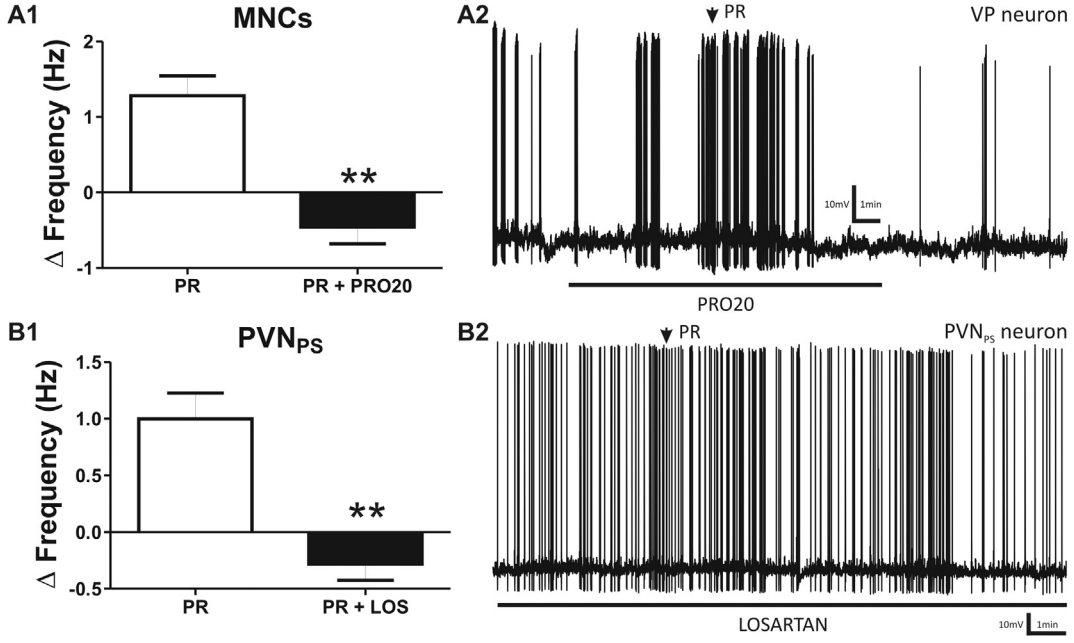

Figure 2: PR effects involve distinct AngII-independent and dependent signaling mechanisms in MNCs and PVN$_{PS}$ neurons. A, Mean Δ frequency (Hz, n = 12 and 5 in PR and PR + PRO20) (**A1**) and sample trace (**A2**) showing that bath application of the PRR-antagonist PRO20 (250 nM, 10 min), prevented PR-evoked excitation in MNCs. **B**, Summary data (n = 12 and 6 in PR and PR + LOS) (**B1**) and representative trace (**B2**) showing that the AT$_1$-R blocker losartan (50 μM, 20 min), blocked PR-evoked excitation in PVN$_{PS}$ neurons. **p < 0.01.

 © 2016 The Author(s). Published by Elsevier GmbH. This is an open access article under the CC BY-NC-ND license (http://creativecommons.org/licenses/by-nc-nd/4.0/).

n = 11; responsive cells: 9/11). To address if this effect was AT_1R-mediated, we repeated this experiment in the presence of both AGT and losartan (50 μM). PR excitatory effect still persisted in this condition (before PR 1.9 ± 0.4 Hz vs. after PR 4.2 ± 1.3 Hz; p = 0.03; n = 9; responsive cells: 8/9).

3.3. PR excitatory effects in MNCs and PVN_{PS} neurons are Ca^{2+}-dependent

It was recently shown that PR application stimulated Ca^{2+} influx in cultured neuroblastoma cells [52]. Thus, to determine if PR excitatory effects in MNCs and PVN_{PS} neurons were Ca^{2+}-dependent, we used two complementary approaches. In a first series of studies, we performed simultaneous patch-clamp electrophysiology and live confocal imaging to determine if PR evoked a change in intracellular Ca^{2+} that preceded the increase in firing activity. As shown in Figure 3, PR application caused a small and slow-developing increase in somatic $[Ca^{2+}]$i in both MNCs (Ca^{2+} peak prior to action potential firing: before PR 1.02 ± 0.01 F/F0 vs. after PR 1.06 ± 0.01 F/F0; p = 0.007; Ca^{2+} area: before PR 388.8 ± 114.6 F/F0*s vs. after PR 1619.4 ± 314.8 F/F0*s, p = 0.005; n = 8) and PVN_{PS} neurons (Ca^{2+} peak: before PR 0.92 ± 0.02 F/F0 vs. after PR 1.07 ± 0.05 F/F0; p = 0.02; Ca^{2+} area: before PR 362.5 ± 83.9 F/F0*s vs. after PR 3646.2 ± 693.9 F/F0*s, p = 0.01, n = 5). The PR-induced elevation in $[Ca^{2+}]$i was accompanied by a slowly developing membrane depolarization, and the Δ$[Ca^{2+}]$i magnitude was positively correlated to the magnitude of the evoked membrane depolarization (r^2: 0.6; p = 0.003). Importantly, the PR-induced slow elevation in $[Ca^{2+}]$i clearly preceded the onset of firing, which then as expected, evoked an abrupt and further increase in $[Ca^{2+}]$i on top of the PR-evoked Δ$[Ca^{2+}]$i (see Figure 3, asterisks). In cases where dendritic processes were sufficiently filled with the Ca^{2+}-sensitive dye, we also observed an increase in dendritic $[Ca^{2+}]$i following PR application (see Figure 3A,B).

Taken together, our simultaneous Ca^{2+} imaging/electrophysiology experiments suggest that the PR-induced increase in $[Ca^{2+}]$i could be an underlying mechanism contributing to the PR excitatory effect in MNCs and PVN_{PS} neurons. To further confirm this, we assessed whether intracellular Ca^{2+} chelation prevented PR excitatory effects. As shown in Figure 3D, PR-evoked increase in firing discharge was abolished when recorded neurons were dialyzed with the Ca^{2+} chelator BAPTA (10 mM) (MNCs; p = 0.2; n = 19; PVN_{PS} neurons: p = 0.5; n = 5).

We next attempted to identify the source of the Ca^{2+} contributing to the PR-mediated effects. The slow-developing kinetics of the PR-evoked increase in $[Ca^{2+}]$i could suggest a slow release from intracellular Ca^{2+} stores as a mechanism mediating PR effects. To determine if the endoplasmic reticulum (ER), a major Ca^{2+} store and regulator of $[Ca^{2+}]$i dynamics in SON and PVN neurons [56], contributed to PR effects, experiments were repeated in slices previously incubated with

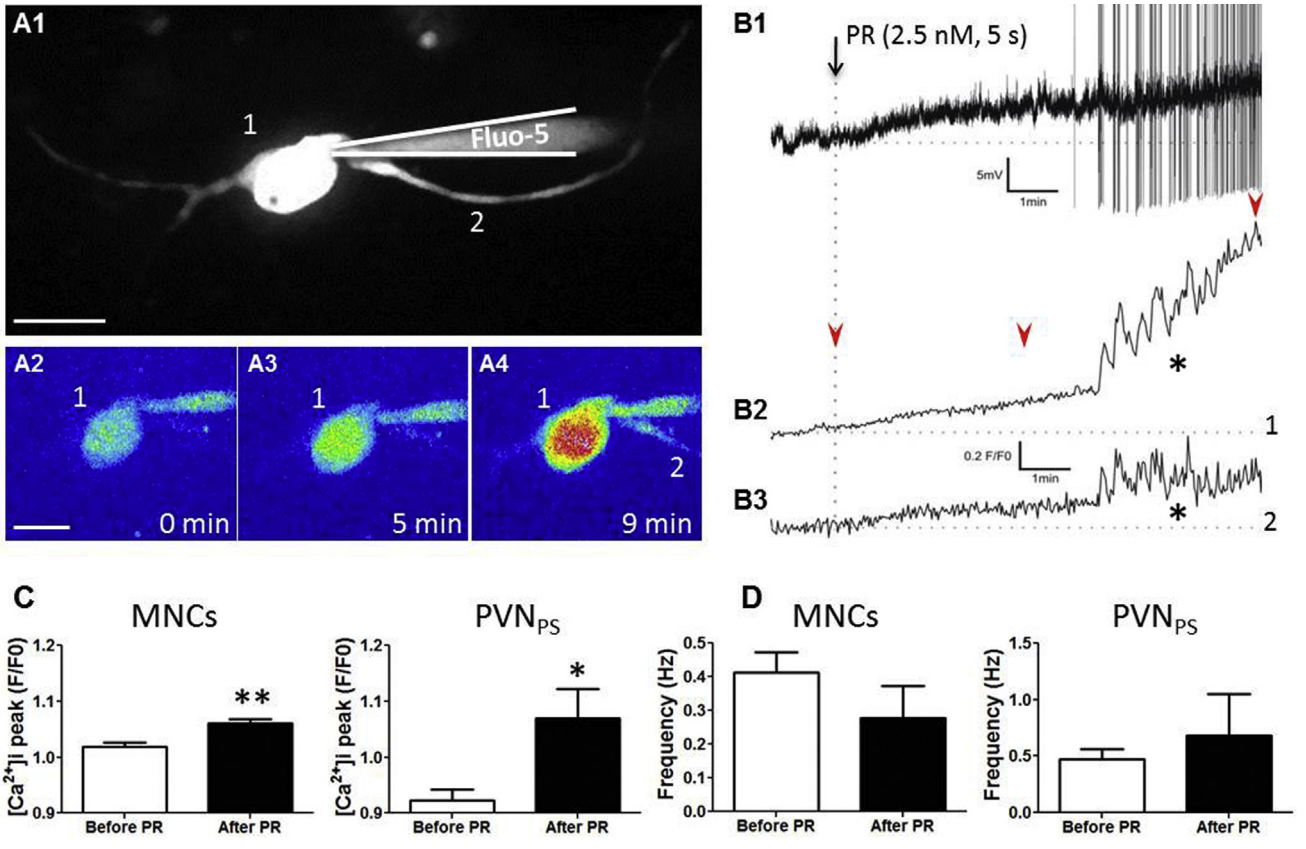

Figure 3: PR effects on MNCs and PVN_{PS} neurons involve an increase in $[Ca^{2+}]$i and are abolished by the Ca^{2+} chelator BAPTA. A, Representative example of an eGFP-VP neuron loaded with the Ca^{2+} indicator Fluo-5F (50 μM) (**A1**). Pseudocolor images showing PR-evoked Ca^{2+} changes over time in that neuron are shown below (**A2**—**A4**). **B**, Sample traces showing simultaneous membrane potential (**B1**) and somatic **(B2)** and dendritic **(B3)** Δ$[Ca^{2+}]$i measurements in the eGFP-VP neuron shown in A, in response to focally-applied PR (5 s, arrow). Arrowheads correspond to the images shown in A2—A4. Note that PR evoked a slow increase in Δ$[Ca^{2+}]$i along with membrane depolarization, which preceded onset of firing and an abrupt action potential-mediated increase in Δ$[Ca^{2+}]$i (asterisks). **C**, Summary data showing mean PR-evoked peak Ca^{2+} changes (F/F0) prior to action potential firing in MNCs ($p < 0.01$, n = 8) and PVN_{PS} neurons ($p < 0.05$, n = 5). **D**, Summary data showing that chelation of intracellular Ca^{2+} with BAPTA (10 mM) in the patch pipette blunted PR excitatory effect in both MNCs ($p > 0.2$, n = 19) and PVN_{PS} neurons ($p > 0.5$, n = 5). Scale bars: 20 μm.

 © 2016 The Author(s). Published by Elsevier GmbH. This is an open access article under the CC BY-NC-ND license (http://creativecommons.org/licenses/by-nc-nd/4.0/).

the SERCA pump inhibitor thapsigargin (3 μM; 45 min). PR application in this condition still triggered an increase in $[Ca^{2+}]i$ (Ca^{2+} peak: before PR 1.03 ± 0.01 F/F0 vs. after PR 1.11 ± 0.02 F/F0; p = 0.003; n = 11), as well as an increase in firing activity (Δ firing rate: 1.2 ± 0.3 Hz; p = 0.007; n = 7). These results suggest that the ER is not a main source of the PR-evoked increase in $[Ca^{2+}]i$.

To determine if PR-mediated effects required an influx of extracellular Ca^{2+}, experiments were repeated in a 0 Ca^{2+} ACSF. In this condition, PR was still able to evoke an increase in firing activity (before PR 1.5 ± 0.3 Hz vs. after PR 5.9 ± 1.3 Hz; p = 0.01; n = 6). These results suggest that the PR-evoked increase in $[Ca^{2+}]i$ does not involve an influx of extracellular Ca^{2+}.

3.4. PR effects involve inhibition of a voltage-gated outward K^+ current in a Ca^{2+}-dependent manner

Voltage-ramp commands (−100 to +40 mV, 28 mV/s) were used to monitor voltage-gated currents in MNCs and PVN_{PS} neurons (Figure 4). Action potentials were blocked by dialyzing neurons with QX314 (5 mM) in the patch pipette. Under these conditions, the ramps evoked predominantly voltage-gated outward currents (Figure 4A). PR application resulted in a significant decrease in the peak magnitude of the elicited outward currents in both MNCs (before PR 2657.8 ± 447.9 pA vs. after PR 2153.9 ± 365.3 pA; p = 0.004; n = 18, 4 of which where eGFP-VP neurons) and PVN_{PS} neurons (before PR 3370.5 ± 796.7 pA vs. after PR 3231.0 ± 769.5 pA; p = 0.02; n = 12). The PR-sensitive current was isolated by digital subtraction of the evoked current before and after PR application (see insets in Figure 4), resulting in a net inward current. The PR-sensitive inward current in MNCs and PVN_{PS} neurons activated at a Vm of −11.2 mV and −10.4 mV respectively, and had a mean peak amplitude of ∼−500 pA and ∼−110 pA (see Figure 4), and a mean peak current density amplitude of 23.1 pA/pF and 2.8 pA/pF, respectively.

Dialyzing neurons with a Cs^+-based internal solution, a broad spectrum K^+ channel blocker, abolished the PR-sensitive inward current (mean peak amplitude: 30.7 ± 34.3 pA; p = 0.2; n = 7). These results indicate that PR is acting by inhibiting a voltage-gated outward K^+ current.

In accordance with the results obtained in current-clamp mode, in MNCs PR failed to inhibit the evoked K^+ currents in the presence of the PRR antagonist, PRO20 (before PR 4591.7 ± 798.9 pA vs. after PR 4529.4 ± 782.4 pA; p = 0.6; n = 9), whereas in PVN_{PS} neurons, PR failed to inhibit the evoked K^+ currents in the presence of losartan (before PR 6658.7 ± 522.7 pA vs. after PR 6379.9 ± 603.6 pA; p = 0.4; n = 8).

Finally, in both neuronal populations, the PR-induced inhibition of outward K^+ currents was abolished by intracellular dialysis with BAPTA (MNCs: p = 0.3; n = 12; PVN_{PS}: p = 0.5; n = 8, Figure 4C,D). In both cases, as shown in Figure 4, a small PR-sensitive outward current was unveiled in the presence of BAPTA.

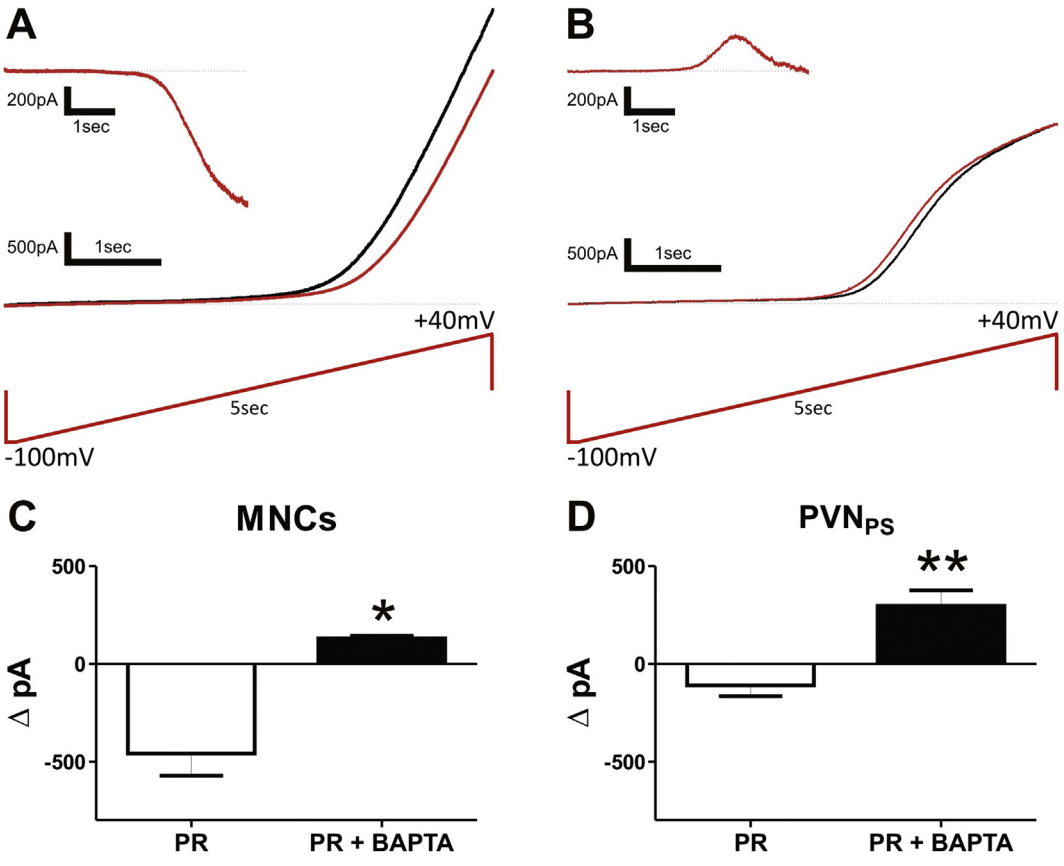

Figure 4: PR inhibits voltage-dependent K^+ currents in a Ca^{2+}-dependent manner. A, Representative example of currents elicited by voltage ramps (−100 mV to +40 mV, 5s) before (black) and after (red) PR application (2.5 nM, 5 s) in an eGFP-VP neuron. Note the decreased magnitude of the outward component in PR. The isolated PR-sensitive current is shown in the inset. **B**, Representative example showing that the PR-mediated inhibition of K^+ currents was abolished in an eGFP-VP neuron dialyzed with BAPTA (10 mM). Note in the inset that the PR-sensitive inward current was absent, while a minor PR-sensitive outward current was unveiled. **C** and **D**, Summary data showing the mean PR-sensitive peak current amplitude in MNCs (**C**) and PVN_{PS} neurons (**D**) in control conditions (n = 18 and 12, respectively) and in cells dialyzed with BAPTA (n = 12 and 8, respectively). **p < 0.01.

 © 2016 The Author(s). Published by Elsevier GmbH. This is an open access article under the CC BY-NC-ND license (http://creativecommons.org/licenses/by-nc-nd/4.0/).

3.5. Prorenin receptor (PRR) immunoreactivity in identified MNCs and PVN_{PS} neurons

To assess the degree of PRR expression and distribution within SON and PVN, we performed confocal immunofluorescence experiments using two different antibodies that target distinct regions of the PRR protein. This was done in conjunction with VP and oxytocin (OT) immunoreactivity, along with fluorescent retrograde tract tracing to identify MNCs and PVN_{PS} neurons, respectively. As shown in Figure 5, a similar PRR immunoreactivity pattern was observed with the two different PRR antibodies tested. PRR immunoreactivity was found in identified VP and OT MNCs and PVN_{PS} neurons within the SON and PVN. A semi-quantitative analysis revealed a significantly stronger PRR immunoreactivity in MNCs ($p < 0.0001$; $n = 116$ and 117 for MNCs and PVN_{PS} neurons, respectively; Figure 5F). Moreover, a stronger PRR immunoreactivity was observed in MNCs of the SON when compared to both neuronal types in the PVN ($n = 153$;

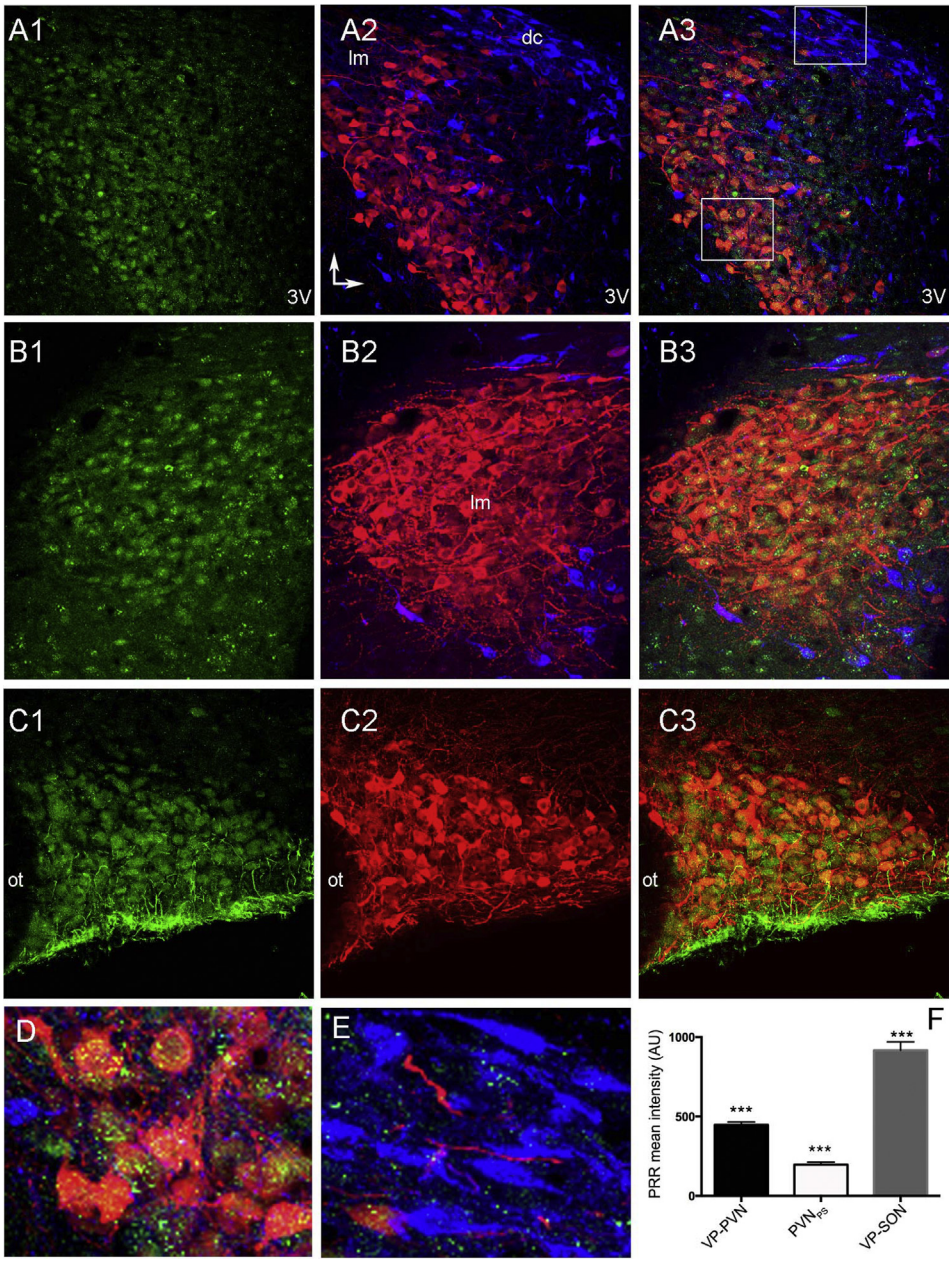

Figure 5: Prorenin receptor (PRR) immunoreactivity in identified MNCs and PVN_{PS} neurons in the SON and PVN. A, PRR immunoreactivity in the PVN (green, antibody generated in Dr. Feng's laboratory, **A1**), in which oxytocin (OT) MNCs (red) and PVN_{PS} neurons (blue) were identified (**A2**). In **A3**, images in A1 and A2 were superimposed, and the areas contained within the white squares are reimaged at higher magnification and displayed in **D**–**E. B**, PRR immunoreactivity in the PVN (green, Abcam antibody, **B1**), in which vasopressin (VP) MNCs (red) and PVN_{PS} neurons (blue) were identified (**B2**). In **B3**, images in B1 and B2 were superimposed. **C**, PRR immunoreactivity in the SON (green, antibody generated in Dr. Feng's laboratory, **C1**), in which both OT and VP neurons were identified (red, **C2**). In **C3**, images in C1 and C2 were superimposed. **F**, Summary data showing mean PRR immunoreactivity intensity in identified VP neurons in the SON and PVN, and PVN_{PS} neurons in the PVN ($n = 153$, 116 and 117 respectively, from 3 rats). ***$p < 0.0001$ vs. all other groups. 3V: third ventricle; dc; dorsal cap; lm: lateral magnocellular subnucleus, ot: optic tract. Scale bars in A–C: 50 μm and D–E: 20 μm. Vertical and horizontal arrows in A2 point dorsally and medially, respectively.

 © 2016 The Author(s). Published by Elsevier GmbH. This is an open access article under the CC BY-NC-ND license (http://creativecommons.org/licenses/by-nc-nd/4.0/).

$p < 0.0001$ vs. both MNCs and PVN_{PS} neurons in the PVN; Figure 5F). PRR immunoreactivity was not limited to MNCs and PVN_{PS} neuronal populations, given that strong PRR staining was also observed in non-labeled neurons throughout the PVN.

4. DISCUSSION

Despite the growing evidence highlighting the importance of the RAS in general, and PRR (one of the newer members of the RAS) in particular, in cardiometabolic control in obesity and hypertension [4,5,7,43,44,46,57], the precise cellular targets and mechanisms underlying central PR/PRR signaling mechanisms remain largely unknown. Thus, the objective of this study was to investigate precise cellular mechanisms by which PR/PRR influence the activity of neurosecretory and presympathetic neurons within the hypothalamic SON and PVN, critical areas implicated in sympatho-humoral regulation by the central RAS. To this end, we used a multidisciplinary approach combining patch-clamp electrophysiology, live confocal imaging and immunohistochemistry. The present study reports several novel findings: 1) PR stimulated firing activity of both neurosecretory and presympathetic PVN neurons; 2) PR effects on both cell types involved binding to PRR (effects were blocked by PRO20). However, while effects on presympathetic neurons were AngII-dependent (blocked by losartan), stimulation of neurosecretory activity was AngII-independent; 3) PR/PRR excitatory effects were Ca^{2+}-dependent, and involved inhibition of a Ca^{2+}-sensitive outward K^{+} current; 4) We found PRR receptor expression both in VP and OT MNCs, and to a lesser degree, in presympathetic PVN neurons.

4.1. PR effects on PVN neuronal activity are cell-type dependent and involve AngII-dependent and -independent pathways

It is now well established that binding of PR to PRR not only mediates formation of AngII via enzymatic conversion of AGT, but it also can lead to activation of a variety of intracellular signaling cascades, including, activation of the mitogen-activated protein kinases p38, ERK 1/2 and downstream targets, such as NADPH oxidase and NFKB [57] among others. Importantly, both AngII-dependent and independent PRR signaling pathways have been linked to the pathogenesis of neurogenic hypertension [37,42–44]. Still, whether these alternative PR/PRR mediated pathways target distinct neuronal substrates and are in turn implicated in mediating particular components of the complex cardiovascular effects reported, including neuro-hormonal release and sympathoexcitation, is still incompletely understood.

Our electrophysiological studies, showing for the first time that PR increased the firing activity of both MNCs and presympathetic PVN neurons, support these neuronal populations as key neuronal substrates mediating central actions of PR/PRR. Using a transgenic rat expressing eGFP driven by the VP promoter [48], we were able to determine that PR/PRR stimulated the firing activity of both VP (eGFP-labeled) and OT neurons (eGFP-negative), the only two neuronal populations present in the SON [26,48]. The fact that PRR affects both OT and VP neurosecretory neurons is also supported by our immunohistochemical studies showing expression of PRR in both neuronal populations. We acknowledge however that PRR staining was not limited to these neuronal populations, and that other PVN neurons involved in cardiometabolic control, such as CRH neurons, could also express PRR. Thus, future studies will be needed to obtain a complete characterization of PRR distribution in the PVN.

Given their wide-ranging influence on fluid/electrolyte/energy balance, body weight, and sympathetic outflow to both cardiovascular- and metabolic-related targets, these three key hypothalamic neuronal populations (neurosecretory OT and VP and presympathetic neurons) play critical roles in cardiovascular and energy balance, and have been implicated in cardiometabolic dysregulation in hypertension and obesity. Taken together, our studies suggest that by modulating their firing activity, PR/PRR constitute critical players within the central RAS to affect cardiometabolic control by the PVN.

Interestingly, PR effects on both MNCs and presympathetic PVN neurons were largely blunted by PRO20, a PRR antagonist that blocks both AngII formation and AngII-independent signaling [52]. Conversely, the AT_1R blocker losartan was effective in blocking PR effects only in presympathetic neurons. Together, these results indicate that PR/PRR effects on MNCs and presympathetic PVN neurons involve AngII-independent and dependent pathways, respectively. The fact that PR effects on two neuronal populations that are anatomically interrelated involved such disparate mechanisms is somewhat unexpected. This could be due, at least in part, to a differential expression of PRR and AT_1Rs between these SON/PVN neuronal types. Previous studies showed that PRR is highly expressed in the SON and PVN, primarily in neurons [37,38], and that its expression is enhanced during hypertension [38,42,44]. However, the distribution of PRR within specific neuronal phenotypes in these regions has not been systematically explored. Our studies support the expression of PRR in neurosecretory VP and OT neurons, and to a lesser degree in presympathetic neurons, indicating that PR can directly act on these distinct neuronal populations. A caveat however, is that while we focally applied PR to these neurons, we cannot completely rule out the possibility that PR may have leaked out in the extracellular space to activate PRRs in other cell populations, such as microglia [58], which may in turn contribute as intermediary cells to the neuronal effects herein described. We did not attempt to assess AT_1R immunoreactivity in this study, given recent reports that questioned the specificity and validity of commercially available AT_1R antibodies [59]. Thus, further studies using alternative experimental approaches will be needed to determine whether a differential expression of AT_1Rs between MNCs and presympathetic neurons contribute to the AngII-independent and dependent mechanisms described in this study.

It is worth mentioning that we found a higher PRR immunoreactivity in VP neurons of the SON compared to those in the PVN, a result that is in line with the stronger PRR effect we reported on the firing activity of SON, compared to MNCs in the PVN.

Another caveat is that endogenous AGT levels, necessary for the formation of AngII by PRR, could be altered in the slice preparation. The fact that we were able to evoke an AngII/AT_1R-mediated effect following PR application in PVN_{PS} neurons would argue against lack of endogenous AGT in our preparation. Still, to rule out that the absence of an AngII-dependent response in MNCs was not due to diminished availability of AGT to this particular neuronal population, we repeated experiments in the presence of exogenously applied AGT. We found that PR effects on MNCs in this condition still persisted, and were unaffected by losartan, further supporting that PR/PRR in MNCs involve an AngII-independent mechanism.

Our results showing that PR/PRR effects on presympathetic PVN neurons were AngII-dependent may seem in apparent conflict with a recent study showing that administration of human prorenin within the PVN elicited an AngII-independent increase in splanchnic, but not renal, sympathetic activity [37]. However, it is important to note that the PVN contains different subpopulations of presympathetic neurons that innervate distinct targets (i.e., RVLM, NTS, spinal cord). Thus, it is possible that PR regulation of sympathetic outflow to selective targets involves distinct subpopulations of PVN presympathetic neurons, which could in turn be differentially modulated by PR.

 © 2016 The Author(s). Published by Elsevier GmbH. This is an open access article under the CC BY-NC-ND license (http://creativecommons.org/licenses/by-nc-nd/4.0/).

The concentration of PR used in this study was within the same range (nM) and even lower than those previously reported [37,52,57]. Importantly, the time course of the effect we observed was similar to those previously reported, with an onset after a few minutes of PR application [37,43]. Moreover, Huber et al. recently reported that a single PR injection within the PVN resulted in a sympathoexcitatory response that remained elevated through the 110 min experimental period [37]. Thus, our results showing an irreversible effect of PR on SON/PVN firing activity, at least within the time period of our recordings, are in agreement with these *in vivo* studies.

4.2. PR/PRR actions in SON/PVN neurons involve modulation of voltage-dependent K^+ channels in a Ca^{2+}-dependent manner

Our simultaneous Ca^{2+} imaging and electrophysiological recordings showed that the PR-mediated slow elevation in intracellular Ca^{2+} preceded the onset of firing. Given the slow kinetics of the Ca^{2+} rise, we initially hypothesized that this increase in Ca^{2+} was due to the slow Ca^{2+} release from the ER, a major source of Ca^{2+} in the SON and PVN [56]. However, we found that depleting the ER Ca^{2+} stores with thapsigargin did not prevented PR effects. We also found that the PR effects persisted in a 0 Ca^{2+} media, indicating that a slow-acting extracellular Ca^{2+} source (e.g., a membrane transporter) or Ca^{2+} channels were also not involved. Thus, it is likely that an alternative intracellular store, such as mitochondria, may serve as a source for the PR-mediated increase in intracellular Ca^{2+}.

We also found that PR inhibited a voltage-gated outward K^+ current, and that chelation of intracellular Ca^{2+} with BAPTA prevented both the inhibition of these outward inhibitory K^+ current, as well as the PR-evoked increase in firing discharge. These results together support the notion that PR/PRR excitatory effects on MNCs and presympathetic neurons involved a slow rise in intracellular Ca^{2+} levels followed by inhibition of a voltage-gated K^+ current, in a Ca^{2+}-dependent fashion. Several Ca^{2+}-dependent K^+ channels are expressed in SON/PVN neurons, which efficiently regulate membrane excitability and firing discharge, including the large conductance BK, and the small conductance SK channels [60–63]. These K^+ channels however, are activated by an increase in intracellular Ca^{2+}. Thus, our studies showing that the PR-mediated increase in Ca^{2+} resulted in inhibition of a K^+ current argues against the involvement of BK and/or SK channels. A Ca^{2+}-dependent suppression of a voltage-gated K^+ current (I_{DAP}) was previously demonstrated in MNCs [64]. Inhibition of this K^+ current following a rise in intracellular Ca^{2+} was shown to underlie a depolarizing after potential (DAP) and to evoke firing activity in MNCs. Another potential target mediating PR/PRR effects in SON/PVN neurons is the M-current (KCNQ2/3), a non-inactivating voltage-gated K^+ current that is also suppressed by increases in intracellular Ca^{2+} [65,66], and was shown to be present in MNCs [67]. Undoubtedly, further studies identifying the precise molecular identity of the K^+ channel underlying PR/PRR actions, as well as the source of Ca^{2+} leading to its inhibition, are warranted.

In summary, we provide here novel evidence that indicates that PR stimulates hypothalamic MNCs and presympathetic PVN neuronal activity via distinct, AngII-independent and dependent mechanisms, respectively, and that these actions involve suppression of a voltage-gated K^+ channel in a Ca^{2+}-dependent manner. Elucidating the basic cellular targets and mechanisms by which PR/PRR regulates neuronal activity within the hypothalamus is fundamental information required to obtain a more comprehensive understanding of how the central RAS influences sympatho-humoral regulation of cardiovascular and metabolic functions, both in health and disease states.

AUTHOR CONTRIBUTIONS

SP carried out the experiments. SP and JES analyzed and interpreted data. JES advised on the experiments and the analysis. SP and JES wrote the manuscript. YF provided the PRR antagonist and antibody, and advised on the writing of the manuscript. All authors have approved the final version of the manuscript and agree to be accountable for all aspects of the work. All persons designated as authors qualify for authorship and all those who qualify for authorship are listed.

ACKNOWLEDGEMENTS

This work was supported by National Institutes of Health grants R01 HL112225 and R01 HL090948 to JES, and in part supported by National Institutes of Health grant R01 HL122770 TO YF.

COMPETING INTERESTS

The authors declare that they have no competing interests.

ABBREVIATIONS

AGT	angiotensinogen
AngII	angiotensin II
AT1R	angiotensin type 1 receptor
eGFP	enhanced green fluorescence protein
ERK1/2	extracellular signal-regulated kinases 1 and 2
LOS	losartan
MAPK	mitogen-activated protein kinases
MNC	magnocellular neurosecretory cell
NTS	nucleus of the solitary tract
OT	oxytocin
PR	prorenin
PRR	prorenin receptor
PVN	paraventricular nucleus
PVN_{PS}	parvocellular presympathetic neuron
RAS	renin-angiotensin system
RVLM	rostral ventrolateral medulla
SFO	subfornical organ
SON	supraoptic nucleus
VP	vasopressin.

REFERENCES

[1] Ganten, D., Hermann, K., Bayer, C., Unger, T., Lang, R.E., 1983. Angiotensin synthesis in the brain and increased turnover in hypertensive rats. Science 221:869–871.

[2] Guyenet, P.G., 2006. The sympathetic control of blood pressure. Nature Reviews Neuroscience 7:335–346.

[3] Reaux, A., Fournie-Zaluski, M.C., David, C., Zini, S., Roques, B.P., Corvol, P., et al., 1999. Aminopeptidase A inhibitors as potential central antihypertensive agents. Proceedings of the National Academy of Sciences United States of America 96:13415–13420.

[4] de Kloet, A.D., Krause, E.G., Woods, S.C., 2010. The renin angiotensin system and the metabolic syndrome. Physiology & Behavior 100:525–534.

[5] Grobe, J.L., Grobe, C.L., Beltz, T.G., Westphal, S.G., Morgan, D.A., Xu, D., et al., 2010. The brain Renin-angiotensin system controls divergent efferent mechanisms to regulate fluid and energy balance. Cell Metabolism 12: 431–442.

 © 2016 The Author(s). Published by Elsevier GmbH. This is an open access article under the CC BY-NC-ND license (http://creativecommons.org/licenses/by-nc-nd/4.0/).

[6] Boustany, C.M., Bharadwaj, K., Daugherty, A., Brown, D.R., Randall, D.C., Cassis, L.A., 2004. Activation of the systemic and adipose renin-angiotensin system in rats with diet-induced obesity and hypertension. American Journal of Physiology, Regulatory, Integrative and Comparative Physiology 287: R943–R949.

[7] Cooper, R., Forrester, T., Ogunbiyi, O., Muffinda, J., 1998. Angiotensinogen levels and obesity in four black populations. ICSHIB investigators. Journal of Hypertension 16:571–575.

[8] Rahmouni, K., Mark, A.L., Haynes, W.G., Sigmund, C.D., 2004. Adipose depot-specific modulation of angiotensinogen gene expression in diet-induced obesity. American Journal of Physiology, Endocrinology and Metabolism 286:E891–E895.

[9] de Kloet, A.D., Krause, E.G., Kim, D.H., Sakai, R.R., Seeley, R.J., Woods, S.C., 2009. The effect of angiotensin-converting enzyme inhibition using captopril on energy balance and glucose homeostasis. Endocrinology 150:4114–4123.

[10] Furuhashi, M., Ura, N., Takizawa, H., Yoshida, D., Moniwa, N., Murakami, H., et al., 2004. Blockade of the renin-angiotensin system decreases adipocyte size with improvement in insulin sensitivity. Journal of Hypertension 22:1977–1982.

[11] Porter, J.P., Anderson, J.M., Robison, R.J., Phillips, A.C., 2003. Effect of central angiotensin II on body weight gain in young rats. Brain Research 959: 20–28.

[12] Porter, J.P., Potratz, K.R., 2004. Effect of intracerebroventricular angiotensin II on body weight and food intake in adult rats. American Journal of Physiology, Regulatory, Integrative and Comparative Physiology 287:R422–R428.

[13] Garrison, R.J., Kannel, W.B., Stokes 3rd, J., Castelli, W.P., 1987. Incidence and precursors of hypertension in young adults: the Framingham Offspring Study. Preventive Medicine 16:235–251.

[14] Lim, K., Burke, S.L., Head, G.A., 2013. Obesity-related hypertension and the role of insulin and leptin in high-fat-fed rabbits. Hypertension 61:628–634.

[15] Prior, L.J., Eikelis, N., Armitage, J.A., Davern, P.J., Burke, S.L., Montani, J.P., et al., 2010. Exposure to a high-fat diet alters leptin sensitivity and elevates renal sympathetic nerve activity and arterial pressure in rabbits. Hypertension 55:862–868.

[16] de Kloet, A.D., Pioquinto, D.J., Nguyen, D., Wang, L., Smith, J.A., Hiller, H., et al., 2014. Obesity induces neuroinflammation mediated by altered expression of the renin-angiotensin system in mouse forebrain nuclei. Physiology & Behavior 136:31–38.

[17] Xiong, X.Q., Chen, W.W., Han, Y., Zhou, Y.B., Zhang, F., Gao, X.Y., et al., 2012. Enhanced adipose afferent reflex contributes to sympathetic activation in diet-induced obesity hypertension. Hypertension 60:1280–1286.

[18] Xue, B., Thunhorst, R.L., Yu, Y., Guo, F., Beltz, T.G., Felder, R.B., et al., 2016. Central renin-angiotensin system activation and inflammation induced by high-fat diet sensitize angiotensin II-elicited hypertension. Hypertension 67: 163–170.

[19] Hilzendeger, A.M., Morgan, D.A., Brooks, L., Dellsperger, D., Liu, X., Grobe, J.L., et al., 2012. A brain leptin-renin angiotensin system interaction in the regulation of sympathetic nerve activity. American Journal of Physiology – Heart and Circulatory Physiology 303:H197–H206.

[20] Xue, B., Yu, Y., Zhang, Z., Guo, F., Beltz, T.G., Thunhorst, R.L., et al., 2016. Leptin mediates high-fat diet sensitization of angiotensin II-elicited hypertension by upregulating the brain renin-angiotensin system and inflammation. Hypertension 67:970–976.

[21] Marchesi, C., Paradis, P., Schiffrin, E.L., 2008. Role of the renin-angiotensin system in vascular inflammation. Trends in Pharmacological Sciences 29: 367–374.

[22] Dange, R.B., Agarwal, D., Masson, G.S., Vila, J., Wilson, B., Nair, A., et al., 2014. Central blockade of TLR4 improves cardiac function and attenuates myocardial inflammation in angiotensin II-induced hypertension. Cardiovascular Research 103:17–27.

[23] Gao, Y., Ottaway, N., Schriever, S.C., Legutko, B., Garcia-Caceres, C., de la Fuente, E., et al., 2014. Hormones and diet, but not body weight, control hypothalamic microglial activity. Glia 62:17–25.

[24] Shi, P., Diez-Freire, C., Jun, J.Y., Qi, Y., Katovich, M.J., Li, Q., et al., 2010. Brain microglial cytokines in neurogenic hypertension. Hypertension 56:297–303.

[25] Thaler, J.P., Guyenet, S.J., Dorfman, M.D., Wisse, B.E., Schwartz, M.W., 2013. Hypothalamic inflammation: marker or mechanism of obesity pathogenesis? Diabetes 62:2629–2634.

[26] Armstrong, W.E., Warach, S., Hatton, G.I., McNeill, T.H., 1980. Subnuclei in the rat hypothalamic paraventricular nucleus: a cytoarchitectural, horseradish peroxidase and immunocytochemical analysis. Neuroscience 5:1931–1958.

[27] Chen, Q.H., Toney, G.M., 2010. In vivo discharge properties of hypothalamic paraventricular nucleus neurons with axonal projections to the rostral ventrolateral medulla. Journal of Neurophysiology 103:4–15.

[28] Porter, J.P., Brody, M.J., 1985. Neural projections from paraventricular nucleus that subserve vasomotor functions. American Journal of Physiology 248: R271–R281.

[29] Woods, S.C., D'Alessio, D.A., 2008. Central control of body weight and appetite. Journal of Clinical Endocrinology & Metabolism 93:S37–S50.

[30] Chee, M.J., Pissios, P., Maratos-Flier, E., 2013. Neurochemical characterization of neurons expressing melanin-concentrating hormone receptor 1 in the mouse hypothalamus. Journal of Comparative Neurology 521:2208–2234.

[31] Ho, J.M., Blevins, J.E., 2013. Coming full circle: contributions of central and peripheral oxytocin actions to energy balance. Endocrinology 154:589–596.

[32] Kublaoui, B.M., Gemelli, T., Tolson, K.P., Wang, Y., Zinn, A.R., 2008. Oxytocin deficiency mediates hyperphagic obesity of Sim1 haploinsufficient mice. Molecular Endocrinology 22:1723–1734.

[33] Perello, M., Raingo, J., 2013. Leptin activates oxytocin neurons of the hypothalamic paraventricular nucleus in both control and diet-induced obese rodents. PLoS One 8:e59625.

[34] Tolson, K.P., Gemelli, T., Meyer, D., Yazdani, U., Kozlitina, J., Zinn, A.R., 2014. Inducible neuronal inactivation of Sim1 in adult mice causes hyperphagic obesity. Endocrinology 155:2436–2444.

[35] McKinley, M.J., Albiston, A.L., Allen, A.M., Mathai, M.L., May, C.N., McAllen, R.M., et al., 2003. The brain renin-angiotensin system: location and physiological roles. International Journal of Biochemistry and Cell Biology 35: 901–918.

[36] Nguyen, G., Delarue, F., Burckle, C., Bouzhir, L., Giller, T., Sraer, J.D., 2002. Pivotal role of the renin/prorenin receptor in angiotensin II production and cellular responses to renin. Journal of Clinical Investigation 109:1417–1427.

[37] Huber, M.J., Basu, R., Cecchettini, C., Cuadra, A.E., Chen, Q.H., Shan, Z., 2015. Activation of the (pro)renin receptor in the paraventricular nucleus increases sympathetic outflow in anesthetized rats. American Journal of Physiology – Heart and Circulatory Physiology 309:H880–H887.

[38] Shan, Z., Shi, P., Cuadra, A.E., Dong, Y., Lamont, G.J., Li, Q., et al., 2010. Involvement of the brain (pro)renin receptor in cardiovascular homeostasis. Circulation Research 107:934–938.

[39] Feldt, S., Batenburg, W.W., Mazak, I., Maschke, U., Wellner, M., Kvakan, H., et al., 2008. Prorenin and renin-induced extracellular signal-regulated kinase 1/2 activation in monocytes is not blocked by aliskiren or the handle-region peptide. Hypertension 51:682–688.

[40] Huang, Y., Wongamorntham, S., Kasting, J., McQuillan, D., Owens, R.T., Yu, L., et al., 2006. Renin increases mesangial cell transforming growth factor-beta1 and matrix proteins through receptor-mediated, angiotensin II-independent mechanisms. Kidney International 69:105–113.

[41] Sakoda, M., Ichihara, A., Kaneshiro, Y., Takemitsu, T., Nakazato, Y., Nabi, A.H., et al., 2007. (Pro)renin receptor-mediated activation of mitogen-activated protein kinases in human vascular smooth muscle cells. Hypertension Research 30:1139–1146.

 © 2016 The Author(s). Published by Elsevier GmbH. This is an open access article under the CC BY-NC-ND license (http://creativecommons.org/licenses/by-nc-nd/4.0/).

[42] Li, W., Peng, H., Cao, T., Sato, R., McDaniels, S.J., Kobori, H., et al., 2012. Brain-targeted (pro)renin receptor knockdown attenuates angiotensin II-dependent hypertension. Hypertension 59:1188—1194.

[43] Zubcevic, J., Jun, J.Y., Lamont, G., Murca, T.M., Shi, P., Yuan, W., et al., 2013. Nucleus of the solitary tract (pro)renin receptor-mediated antihypertensive effect involves nuclear factor-kappaB-cytokine signaling in the spontaneously hypertensive rat. Hypertension 61:622—627.

[44] Li, W., Peng, H., Mehaffey, E.P., Kimball, C.D., Grobe, J.L., van Gool, J.M., et al., 2014. Neuron-specific (pro)renin receptor knockout prevents the development of salt-sensitive hypertension. Hypertension 63:316—323.

[45] de Kloet, A.D., Pati, D., Wang, L., Hiller, H., Sumners, C., et al., 2013. Angiotensin type 1a receptors in the paraventricular nucleus of the hypothalamus protect against diet-induced obesity. Journal of Neuroscience 33: 4825—4833.

[46] Tan, P., Shamansurova, Z., Bisotto, S., Michel, C., Gauthier, M.S., Rabasa-Lhoret, R., et al., 2014. Impact of the prorenin/renin receptor on the development of obesity and associated cardiometabolic risk factors. Obesity (Silver Spring) 22:2201—2209.

[47] Wu, C.H., Mohammadmoradi, S., Thompson, J., Su, W., Gong, M., Nguyen, G., et al., 2016. Adipocyte (Pro)renin-receptor deficiency induces lipodystrophy, liver steatosis and increases blood pressure in male mice. Hypertension 68: 213—219.

[48] Ueta, Y., Fujihara, H., Serino, R., Dayanithi, G., Ozawa, H., Matsuda, K., et al., 2005. Transgenic expression of enhanced green fluorescent protein enables direct visualization for physiological studies of vasopressin neurons and isolated nerve terminals of the rat. Endocrinology 146:406—413.

[49] Son, S.J., Filosa, J.A., Potapenko, E.S., Biancardi, V.C., Zheng, H., Patel, K.P., et al., 2013. Dendritic peptide release mediates interpopulation crosstalk between neurosecretory and preautonomic networks. Neuron 78:1036—1049.

[50] Potapenko, E.S., Biancardi, V.C., Florschutz, R.M., Ryu, P.D., Stern, J.E., 2011. Inhibitory-excitatory synaptic balance is shifted toward increased excitation in magnocellular neurosecretory cells of heart failure rats. Journal of Neurophysiology 106:1545—1557.

[51] Stern, J.E., 2001. Electrophysiological and morphological properties of preautonomic neurones in the rat hypothalamic paraventricular nucleus. Journal of Physiology 537:161—177.

[52] Li, W., Sullivan, M.N., Zhang, S., Worker, C.J., Xiong, Z., Speth, R.C., et al., 2015. Intracerebroventricular infusion of the (Pro)renin receptor antagonist PRO20 attenuates deoxycorticosterone acetate-salt-induced hypertension. Hypertension 65:352—361.

[53] Sonner, P.M., Lee, S., Ryu, P.D., Lee, S.Y., Stern, J.E., 2011. Imbalanced K^+ and Ca^{2+} subthreshold interactions contribute to increased hypothalamic presympathetic neuronal excitability in hypertensive rats. Journal of Physiology 589:667—683.

[54] Stern, J.E., Potapenko, E.S., 2013. Enhanced NMDA receptor-mediated intracellular calcium signaling in magnocellular neurosecretory neurons in heart failure rats. American Journal of Physiology, Regulatory, Integrative and Comparative Physiology 305:R414—R422.

[55] Biancardi, V.C., Campos, R.R., Stern, J.E., 2010. Altered balance of gamma-aminobutyric acidergic and glutamatergic afferent inputs in rostral ventrolateral medulla-projecting neurons in the paraventricular nucleus of the hypothalamus of renovascular hypertensive rats. Journal of Comparative Neurology 518:567—585.

[56] Dayanithi, G., Forostyak, O., Ueta, Y., Verkhratsky, A., Toescu, E.C., 2012. Segregation of calcium signalling mechanisms in magnocellular neurones and terminals. Cell Calcium 51:293—299.

[57] Peng, H., Li, W., Seth, D.M., Nair, A.R., Francis, J., Feng, Y., 2013. (Pro)renin receptor mediates both angiotensin II-dependent and -independent oxidative stress in neuronal cells. PLoS One 8:e58339.

[58] Shi, P., Grobe, J.L., Desland, F.A., Zhou, G., Shen, X.Z., Shan, Z., et al., 2014. Direct pro-inflammatory effects of prorenin on microglia. PLoS One 9:e92937.

[59] Herrera, M., Sparks, M.A., Alfonso-Pecchio, A.R., Harrison-Bernard, L.M., Coffman, T.M., 2013. Lack of specificity of commercial antibodies leads to misidentification of angiotensin type 1 receptor protein. Hypertension 61:253—258.

[60] Bourque, C.W., Randle, J.C., Renaud, L.P., 1985. Calcium-dependent potassium conductance in rat supraoptic nucleus neurosecretory neurons. Journal of Neurophysiology 54:1375—1382.

[61] Chen, Q.H., Toney, G.M., 2009. Excitability of paraventricular nucleus neurones that project to the rostral ventrolateral medulla is regulated by small-conductance Ca^{2+}-activated K^+ channels. Journal of Physiology 587:4235—4247.

[62] Greffrath, W., Martin, E., Reuss, S., Boehmer, G., 1998. Components of after-hyperpolarization in magnocellular neurones of the rat supraoptic nucleus in vitro. Journal of Physiology 513(Pt 2):493—506.

[63] Teruyama, R., Armstrong, W.E., 2005. Enhancement of calcium-dependent after potentials in oxytocin neurons of the rat supraoptic nucleus during lactation. Journal of Physiology 566:505—518.

[64] Li, Z., Hatton, G.I., 1997. Reduced outward K^+ conductances generate depolarizing after-potentials in rat supraoptic nucleus neurones. Journal of Physiology 505(Pt 1):95—106.

[65] Adams, P.R., Brown, D.A., Constanti, A., 1982. M-currents and other potassium currents in bullfrog sympathetic neurones. Journal of Physiology 330: 537—572.

[66] Selyanko, A.A., Brown, D.A., 1996. Intracellular calcium directly inhibits potassium M channels in excised membrane patches from rat sympathetic neurons. Neuron 16:151—162.

[67] Zhang, W., Wang, D., Liu, X.H., Kosala, W.R., Rajapaksha, J.S., Fisher, T.E., 2009. An osmosensitive voltage-gated K^+ current in rat supraoptic neurons. European Journal of Neuroscience 29:2335—2346.

 © 2016 The Author(s). Published by Elsevier GmbH. This is an open access article under the CC BY-NC-ND license (http://creativecommons.org/licenses/by-nc-nd/4.0/).